Acclimation of leaf respiration consistent with optimal photosynthetic capacity

Han Wang[1,2*], Owen K. Atkin[3,4], Trevor F. Keenan[5,6], Nicholas G. Smith[7], Ian J. Wright[8], Keith J. Bloomfield[9], Jens Kattge[10,11], Peter B. Reich[12,13] and I. Colin Prentice[1,8,14]

[1] Ministry of Education Key Laboratory for Earth System Modelling, Department of Earth System Science, Tsinghua University, Beijing 100084, China

[2] Joint Centre for Global Change Studies, Beijing 100875, China

[3] Division of Plant Sciences, Research School of Biology, The Australian National University, Canberra, ACT 2601, Australia

[4] Australian Research Council Centre of Excellence in Plant Energy Biology, Research School of Biology, The Australian National University, Canberra, ACT 2601, Australia

[5] Department of Environmental Science, Policy and Management, UC Berkeley, Berkeley, CA, USA

[6] Climate and Ecosystem Sciences Division, Lawrence Berkeley National Laboratory, Berkeley, CA, USA

[7] Department of Biological Sciences, Texas Tech University, Lubbock, TX, USA

[8] Department of Biological Sciences, Macquarie University, NSW 2109, Australia

[9] Department of Life Sciences, Imperial College London, Silwood Park Campus, Buckhurst Road, Ascot SL5 7PY, UK

[10] Max Planck Institute for Biogeochemistry, Jena, Germany

[11] German Center for Integrative Biodiversity Research Halle-Jena-Leipzig, Leipzig, Germany

[12] Department of Forest Resources, University of Minnesota, St. Paul, MN 55108, USA

[13] Hawkesbury Institute for the Environment, Western Sydney University, Penrith, NSW 2753, Australia

[14] AXA Chair of Biosphere and Climate Impacts, Department of Life Sciences, Imperial College London, Silwood Park Campus, Buckhurst Road, Ascot SL5 7PY, UK

*Contact Information

Han Wang: wanghan_sci@yahoo.com

Running Title (A short running title of less than 45 characters including spaces)

optimal acclimation of leaf dark respiration

Abstract

Plant respiration is an important contributor to the proposed positive global carbon-cycle feedback to climate change. However, as a major component, leaf mitochondrial ('dark') respiration (R_d) differs among species adapted to contrasting environments and is known to acclimate to sustained changes in temperature. No accepted theory explains these phenomena or predicts their magnitude. Here we propose that the acclimation of R_d follows an optimal behaviour related to the need to maintain long-term average photosynthetic capacity (V_{cmax}) so that available environmental resources can be most efficiently used for photosynthesis. To test this hypothesis, we extend photosynthetic co-ordination theory to predict the acclimation of R_d to growth temperature via a link to V_{cmax}, and compare predictions to a global set of measurements from 112 sites spanning all terrestrial biomes. This extended co-ordination theory predicts that field-measured R_d should increase by 3.7% and V_{cmax} by 5.5% per degree increase in growth temperature. These acclimated responses to growth temperature are less steep than the corresponding instantaneous responses, which increase 8.1% and 9.9% per degree of measurement temperature for R_d and V_{cmax}, respectively. Data-fitted regression slopes proved indistinguishable from the values predicted by our theory, and smaller than the instantaneous slopes. Theory and data are also shown to agree that the basal rates of both R_d and V_{cmax} assessed at 25˚C decline by ~ 4.4% per degree increase in growth temperature. These results provide a parsimonious general theory for R_d acclimation to temperature that is simpler – and potentially more reliable – than the plant functional type-based leaf respiration schemes currently employed in most ecosystem and land-surface models.

Keywords (6-10)

Leaf respiration, optimality, carboxylation capacity (V_{cmax}), acclimation, land-surface model

Introduction

Land plant respiration is a major component of the carbon cycle, releasing *ca.* 60 Pg C yr^{-1} to the atmosphere: six times more than anthropogenic CO_2 emissions from all sources combined (Ciais et al., 2014). About half is due to mitochondrial respiration in leaves (Atkin, Scheurwater, & Pons, 2007), which is usually called 'dark' respiration (R_d) since it is most easily measured in darkened leaves; mitochondrial respiration continues in the light, although at a reduced rate (Tcherkez et al., 2017). Leaf respiration is closely coupled with photosynthetic activity (Hoefnagel, Atkin, & Wiskich, 1998; Noguchi & Yoshida, 2008; O'Leary, Asao, Millar, & Atkin, 2019; Tcherkez, 2012; Wright et al., 2004). As described by the standard biochemical model of photosynthesis (Farquhar, von Caemmerer, & Berry, 1980), the instantaneous rate of photosynthesis by C_3 plants is limited either by the capacity of the enzyme Ribulose-1,5-bisphosphate (RuBP) carboxylase/oxygenase (Rubisco) for the carboxylation of RuBP (V_{cmax}), or by the rate of electron transport for the regeneration of RuBP, which depends on absorbed light and the electron transport capacity (J_{max}). R_d of fully developed leaves is used to support metabolic processes including protein turnover, phloem loading, the maintenance of ion gradients between cellular compartments, nitrate reduction, and the turnover of phospholipid membranes. Among these, protein turnover is the largest contributor to variation in R_d. Given that Rubisco is a substantial fraction of total leaf protein, R_d is expected to scale closely with V_{cmax}, which sets the daily maximum photosynthetic rate achieved by leaves under natural growing conditions (Amthor, 2000; Atkin, Millar, Gardeström, & Day, 2000; Bouma, 2005; Cannell & Thornley, 2000; O'Leary et al., 2019). R_d is commonly assumed in Land Surface Models (LSMs) to be proportional either to V_{cmax} or, alternatively, to area-based leaf nitrogen content (N_{area}) (Rogers, 2014).

Leaf respiration is enzyme-catalysed and therefore temperature-dependent. On a time scale of minutes to hours, R_d responds to leaf temperature near-exponentially and is determined principally by the temperature dependence of the reaction rates of multiple enzymes involved in various respiratory pathways in the cytosol and mitochondria (Atkin, Bruhn, & Tjoelker, 2005; Atkin & Tjoelker, 2003). We refer to this observed, composite temperature response as the "instantaneous" response. Because of this temperature response of R_d, it has been proposed that global warming will increase

plant respiration and accelerate climate change (Cox, Betts, Jones, Spall, & Totterdell, 2000; Huntingford et al., 2013). However, the magnitude of this positive feedback remains unclear. It depends on the sensitivity of plant respiration to temperature changes over longer time scales, which – as many experiments have shown – is damped, relative to the short-term response, by acclimation (Atkin & Tjoelker, 2003; Reich et al., 2016; Scafaro et al., 2017). The longer-term response of plant respiration to the prevailing growth temperature is also manifest in spatial patterns of leaf R_d (Atkin et al., 2015; Slot & Kitajima, 2015), which show a far less steep pole-to-equator gradient than would be expected from the instantaneous response – a consequence of both acclimation (plastic responses) and adaptation, i.e. differences among genotypes and species adapted to contrasting environments. Vanderwel et al. (2015) moreover demonstrated consistency between the observed spatial pattern of R_d and the acclimation of leaf R_d over time. Pervasive long-term acclimation of respiration implies a weaker positive carbon-climate feedback than is implied by the instantaneous temperature response (Huntingford et al., 2017; Reich et al., 2016; Smith, Malyshev, Shevliakova, Kattge, & Dukes, 2016). Neglecting the acclimation of plant respiration to temperature in LSMs may therefore be a major source of bias in Earth System model predictions (Huntingford et al., 2017; Smith et al., 2016).

Quantitative explanations and predictions of the acclimation and adaptation of leaf R_d to temperature are still lacking. Conclusions from empirical studies alone (Wright et al., 2006) are insufficient to address the underlying causality; a firmer theoretical basis is essential to build confidence in carbon-cycle predictions (Prentice, Liang, Medlyn, & Wang, 2015). Here we propose a theoretical framework for the acclimation of leaf R_d based on a few key hypotheses. We first assume acclimation of V_{cmax} (Step 1 in Fig. 1) via the 'co-ordination hypothesis', which states that V_{cmax} assessed at growth temperature ($V_{cmax,tg}$) has a general tendency to adjust to average daytime conditions so that the electron transport- and Rubisco-limited photosynthetic rates (A_J, A_c) are co-limiting (Chen, Reynolds, Harley, & Tenhunen, 1993; Haxeltine & Prentice, 1996; Maire et al., 2012) (that is, $A_J \approx A_c$). Co-limitation is optimal in an eco-evolutionary sense because any other outcome would either incompletely exploit available light, or require additional respiration to maintain excess amounts of Rubisco. This hypothesis explained 64% of field-measured $V_{cmax,tg}$ variability in C_3 plants across different biomes, and has been used with success to predict global patterns of primary production (Smith,

Keenan, Prentice, Wang, Wright, Niinemets, Crous, Domingues, Guerrieri, Yoko Ishida, et al., 2019; Wang et al., 2017). Second, the various metabolic functions of R_d in mature leaves are assumed to be tightly coupled to V_{cmax} (Step 3 in Fig. 1) – implying a close link between the acclimation of V_{cmax} and R_d. We test this hypothesis later, alongside the alternative hypothesis that R_d depends on N_{area}. To simplify the theoretical framework and mathematical derivations, we (a) disregard any possible differences in the instantaneous thermal responses of R_d and V_{cmax} among species and across sites (Steps 2 and 4 in Fig 1), and (b) assume infinite mesophyll conductance and non-limiting electron-transport capacity (Keenan et al., 2016; Togashi et al., 2018; Wang, Prentice, & Davis, 2014). Although uncertainties are thereby inevitably introduced, these simplifications allow us to test first-order effects at a global scale, appropriately for the potential improvement of LSMs.

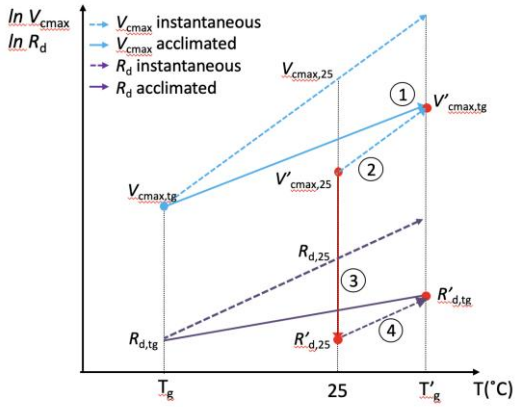

Figure 1: Schematic of the thermal sensitivities of V_{cmax} and leaf R_d. Step 1: The "co-ordination hypothesis" predicts a positive response of V_{cmax} (β_{aV}) to growth temperature. Due to increasing Rubisco oxygenation relative to carboxylation, a higher V_{cmax} is required to achieve the optimal photosynthetic rate at higher temperatures. Step 2: When temperature increases, the value of V_{cmax} achieved through the instantaneous response of Rubisco (β_{iV}) is super-optimal. Consequently, the amount of Rubisco (indexed by V_{cmax} at the standard reference temperature of 25˚C) must be "down-regulated" from $V_{cmax,25}$ to $V'_{cmax,25}$. Step 3: We hypothesize that respiratory and photosynthetic capacities are linked such that $\beta_{qV} = \beta_{qR}$. Leaf $R'_{d,25}$ at growth temperature is then a fraction of $V'_{cmax,25}$. Step 4: Just as for V_{cmax}, leaf $R'_{d,25}$ at the new growth temperature is lower than $R_{d,25}$ at the original growth temperature, implying an acclimated/adapted thermal response (β_{aR}) that is less steep than the instantaneous response (β_{iR}).

Materials and methods

Quantitative predictions

Based on the simplifying assumption that leaf R_d adjusts over time primarily to maintain the turnover of Rubisco and other enzymes involved in the Calvin cycle, we start from the premise that at the prevailing growth temperature (T_g), the acclimated $R_{d,tg}$ is proportional to acclimated $V_{cmax,tg}$:

$$R_{d,tg} = b_{tg}\, V_{cmax,tg} \quad (1)$$

while recognizing that the proportionality factor b_{tg} could vary with environmental conditions. We therefore first focus on quantitative prediction of the optimal thermal acclimation of $V_{cmax,tg}$.

Step 1: optimal $V_{cmax,tg}$ and its thermal acclimation based on the coordination hypothesis

We hypothesize that V_{cmax} of leaves at any canopy level acclimates to the current environment in such a way that the Rubisco-limited (increasing with V_{cmax}) and electron transport-limited (increasing with absorbed PPFD) photosynthetic rates tend to converge. This is the 'strong form' of the coordination hypothesis (Chen et al., 1993; Haxeltine & Prentice, 1996; Maire et al., 2012), contrasting with a 'weak form' that assumes that the total metabolic N content of the leaf is prescribed so that only the allocation of N to carboxylation versus electron transport capacities is optimized. In response to environmental variations, the coordination hypothesis predicts vertical variation of $V_{cmax,tg}$ within the canopy, geographic variation among sites, and temporal variations with atmospheric CO_2 concentration and climate (Haxeltine & Prentice, 1996; Smith, Keenan, Prentice, Wang, Wright, Niinemets, Crous, Domingues, Guerrieri, Ishida, et al., 2019; Terrer et al., 2018). Thus, under field conditions the coordination hypothesis predicts that:

$$V_{cmax,tg} \approx \varphi_0\, I_{abs}\, (\chi\, c_a + K) \,/\, (\chi\, c_a + 2\Gamma^*) \quad (2)$$

where φ_0 is the intrinsic quantum efficiency of photosynthesis (mol mol^{-1}); I_{abs} is the PPFD absorbed by the leaf (µmol m^{-2} s^{-1}); χ is the ratio of leaf-internal to ambient partial pressure of CO_2 (Pa Pa^{-1}); c_a is the ambient partial pressure of CO_2 (Pa); Γ^* is

the photorespiratory compensation point (Pa); and K is the effective Michaelis-Menten coefficient of Rubisco (Pa). Γ^* and K are temperature-dependent following Arrhenius relationships as measured e.g. by Bernacchi et al. (2001). Acknowledging that Rubisco kinetics traits vary both within and among species, we applied various Rubisco catalytic constants (the Michaelis–Menten coefficients for carboxylation and oxygenation, and the Rubisco specificity factor) provided by (Galmés, Hermida-Carrera, Laanisto, & Niinemets, 2016) to estimate the uncertainties (± 1 s.d.) in K, Γ^* and their instantaneous thermal responses.

The least-cost hypothesis (Prentice, Dong, Gleason, Maire, & Wright, 2014; Wang et al., 2017) predicts optimal χ to be a function of growing-season mean values of temperature (T_g; K), vapour pressure deficit (D; Pa) and elevation (z; m). These predictions are quantitatively supported by worldwide measurements of χ across species and biomes (Wang et al., 2017). Equation (2) then yields estimates of V_{cmax} given χ and field-relevant average values of c_a (Pa), temperature (K) and PPFD (µmol m^{-2} s^{-1}).

We define temperature sensitivities (β) of various quantities as fractional increases per degree. The fractional sensitivity of $V_{cmax,tg}$ to temperature after acclimation (β_{aV}) can be deduced by differentiating equation (2) with respect to T_g:

$$\beta_{aV} = (\partial V_{cmax,tg}/\partial T_g) / V_{cmax,tg} = \partial \ln V_{cmax,tg}/\partial T_g$$

$$= \partial \ln (\chi c_a + K)/\partial T_g - \partial \ln (\chi c_a + 2\Gamma^*)/\partial T_g \quad (3)$$

Evaluating equation (3) under standard conditions (T_g = 298 K, D = 1 kPa, z = 0, c_a = 40 Pa) yields β_{aV} = 5.5 ± 0.3 % K^{-1}. This value derives primarily from the sensitivities of K and Γ^* to temperature (8.5% K^{-1} and 5.4% K^{-1}, respectively), which depend on their activation energies (Bernacchi et al., 2001), and to a lesser extent from the sensitivity of χ to temperature (0.9% K^{-1}).

Step 2: optimal $V_{cmax,25}$ and its thermal acclimation

Described by a modified Arrhenius function (Kattge & Knorr, 2007), the instantaneous temperature response of V_{cmax} to temperature provides a link between $V_{cmax,tg}$ and $V_{cmax,25}$:

$$V_{cmax,tg} = V_{cmax,25} \times f_v$$

where

$$f_v = e^{Ha\,(Tg-298.15)\,/\,298.15TgR} \times [1+e^{(298.15\Delta S - Hd)\,/\,(298.15R)}] \,/\, [1+e^{(Tg\Delta S - Hd)\,/\,(TgR)}] \quad (4)$$

where H_a is the activation energy (71 513 J mol^{-1}), R is the universal gas constant (8.314 J mol^{-1} K^{-1}), T_{ref} = 298.15 K, H_d is the deactivation energy (200 000 J mol^{-1}), and ΔS is an entropy term (J mol^{-1} K^{-1}), which can be calculated using a linear relationship with T_g from (Kattge & Knorr, 2007) with a slope of 1.07 J mol^{-1} K^{-2} and an intercept of 668.39 J mol^{-1} K^{-1}.

To estimate the uncertainties (± 1 s.d.) in Rubisco kinetics, We applied various maximum carboxylase turnover rate provided by Galmés, Kapralov, Copolovici, Hermida-Carrera, and Niinemets (2015). Equation (4) then generates an instantaneous response of V_{cmax} to temperature with a high sensitivity β_{iV} of 9.9 ± 1.4 % K^{-1}, and allows β_{qV} to be derived as:

$$\begin{aligned} \beta_{qV} &= \partial \ln V_{cmax,25} / \partial T_g \\ &= \partial \ln V_{cmax,tg} / \partial T_g - \partial \ln f_v / \partial T_g \\ &= \beta_{aV} - \beta_{iV} \\ &= -4.4 \pm 1.4\ \%\ K^{-1} \end{aligned} \quad (5)$$

We can thus break down the acclimated temperature sensitivity of $V_{cmax,tg}$ (β_{aV}) into the instantaneous sensitivity of Rubisco to temperature changes (β_{iV}) and the acclimated sensitivity (β_{qV}) of the amount of Rubisco (as indexed by $V_{cmax,25}$, the catalytic activity of Rubisco at 25˚C) to growth temperature.

Step 3: optimal $R_{d,25}$ and its thermal acclimation based on the link to $V_{cmax,25}$

In commonly used photosynthesis models, leaf $R_{d,25}$ is assumed proportional to $V_{cmax,25}$ with the ratio given as 0.011 (Farquhar et al., 1980) or 0.015 (Collatz, Ball, Grivet, & Berry, 1991). This assumption implies that $R_{d,25}$ is related to $V_{cmax,25}$ by a constant factor b_{25}:

$$R_{d,25} = b_{25}\, V_{cmax,25} \quad (6)$$

and thus also that $\beta_{qV} = \beta_{qR}$ (Figure 1).

We test this key assumption in parallel empirical analyses. The effects of other potential influences, including leaf mass per area, leaf nitrogen content and soil properties, on $R_{d,25}$ are also tested.

Step 4: optimal $R_{d,gt}$ and its thermal acclimation

Heskel et al. (2016) provided an empirical formula to estimate R_d at 25˚C:

$$\ln R_{d,25} = a + 0.1012 \times 25 - 0.0005 \times 25^2 \quad (7)$$

where a is an empirical constant varying among biomes, representing the natural logarithm of the value of R_d extrapolated to 0°C. The instantaneous response of R_d to temperature (β_{iR}) as given by Heskel et al. (2016) is 8.1% K^{-1} at the mean T_g of the data. β_{iR} is slightly smaller than β_{iV}, and leads to a response of parameter b_{tg} in equation (1) given by the difference between β_{iR} and β_{iV} (β_b = –1.8% K^{-1}). This then generates the predictions β_{qR} = –4.4% K^{-1} and β_{aR} = 3.7% K^{-1}.

Using other instantaneous thermal response curves (for example, equations 1 and 3 in Atkin et al. (2015), equation 1 in (Reich et al., 2016), and equation 1 in Kattge and Knorr (2007)) yielded slightly different instantaneous responses of R_d and V_{cmax} to temperature. However, those changes also effect temperature adjustment we applied in the parallel empirical analysis, and have little influence on our testing. We therefore report only the results from the equations as described above.

Empirical analyses

Photosynthesis and respiration data

We combined two R_d datasets: the global respiration (GlobResp) and leaf carbon exchange (LCE) datasets. GlobResp (Atkin et al., 2015) contains measurements of leaf R_d, V_{cmax}, N_{area} and leaf mass per area (LMA) from 899 species at 100 locations across the major biomes and continents, including data from an earlier compilation by Wright et al. (2004). LCE (Smith & Dukes, 2017a) contains field measurements of leaf carbon exchange and chemical traits from 98 species at 12 locations spanning 53˚ latitude in North and Central America (Fig. S1). Replicated measurements in LCE on the same species and site were averaged. Juvenile samples were excluded. Leaf R_d measurements in both datasets followed the same protocol. Both were taken on fully expanded leaves

in daytime after a period of dark adjustment. V_{cmax} values in GlobResp were estimated by the 'one-point method' (De Kauwe et al., 2016) whereas those in LCE were estimated from full A–c_i curves. With a global dataset of A–c_i curves (564 species from 46 field sites, covering a range of plant functional types), De Kauwe et al. (2016) showed that 'the one-point method' can provide a robust approach to expand the available set of field measurements on V_{cmax}. We present analyses based on the combined datasets as the main results in this paper. However, given that Burnett, Davidson, Serbin, and Rogers (2019) recently showed that the one-point method may underestimate V_{cmax}, we also analysed each dataset separately. The results are given in the Supplementary Information.

We indexed T_g by the mean temperature during the thermal growing season with temperatures above 0˚C ($mGDD_0$) (Harrison et al., 2010). V_{cmax} and R_d values in both datasets were provided with information about measurement leaf temperatures. V_{cmax} and R_d values were adjusted both to $mGDD_0$ and to 25˚C using the relevant instantaneous responses, as given in Heskel et al. (2016) and Kattge and Knorr (2007), respectively.

A global climatology of monthly temperature provided by the Climatic Research Unit at a grid resolution of 10 arc minutes (CRU CL2.0) (New, Hulme, & Jones, 2000) was used to provide estimates of $mGDD_0$ for each location. Thermal acclimation of R_d should in principle apply to both C_3 and C_4 plants, but our theoretical prediction of V_{cmax} acclimation here is developed for C_3 plants, and we did not include C_4 species in our analysis.

Statistical analysis

The theoretical framework proposed here includes a series of quantitative predictions. Statistical analysis focused on testing the agreement between these theoretical predictions and data. To test our predictions of β_a and β_q quantitatively, the R_d and V_{cmax} data (assessed at $mGDD_0$ and 25˚C) were first normalized with estimates of the site-mean PPFD absorbed by leaves ($PPFD_L$: see Dong et al. (2017) before performing Ordinary Least Squares (OLS) regression against growth temperature. This normalization is appropriate because V_{cmax} is both predicted (equation 2) and observed (Niinemets & Keenan, 2012) to vary in proportion to PPFD. If it were omitted, the

positive effect of PPFD on R_d and V_{cmax} would contribute to the fitted slope of $mGDD_0$ due to the correlation between those two variables (Fig. S2).

$PPFD_L$ was devised to deal with the fact that field-measured photosynthetic trait data reflect leaves developed at a range of irradiances at different levels in the canopy. $PPFD_L$ is estimated from growing-season total incident PPFD at the top of the canopy ($PPFD_0$) as follows:

$$PPFD_L \approx f\ PPFD_0/L \quad (8)$$

where f is the fraction of incident PPFD absorbed by the canopy (obtained from SeaWiFS data (Gobron et al., 2006)) and L is the leaf area index estimated from Beer's law:

$$L \approx -(1/k) \ln (1 - f) \quad (9)$$

with k = 0.5 (Dong, Prentice, Evans, et al., 2017). $PPFD_0$ was calculated from CRU CL2.0 data using the SPLASH model (Davis et al., 2017).

We applied OLS linear regression of normalized and natural log-transformed R_d and V_{cmax} values against $mGDD_0$ using all-species and site-mean data, respectively. To check the impact of the PPFD normalization, we also performed regressions without it. We additionally applied mixed-effects models with species or sites contributing random effects. To test the uncertainty introduced by applying a single set of instantaneous responses, whereas different kinetics responses might arise among species and sites, we conducted a further OLS regression by using a subset of the dataset when R_d and V_{cmax} were measured at a leaf temperature that differs from 25˚C or growth temperature less than 1˚C.

To test the key assumption that $R_{d,25}$ is mainly determined by $V_{cmax,25}$, we applied OLS linear regression of R_d versus V_{cmax} (standardized to 25˚C and separately to $mGDD_0$, without transformation) to estimate b_{25} and b directly from the fitted slopes. We also included LMA and soil pH as additional predictors in the regression described above. LMA carries information on the structural component of plant leaves. Broadly speaking, higher soil pH and cation exchange capability indicate higher soil fertility (Jenny, 1994; Sinsabaugh & Follstad Shah, 2012), and pH has been shown to influence χ (Wang et

al., 2017). These covariates were selected to test any potential influences of leaf structure and soil nutrient availability on $R_{d,25}$. An estimate of soil pH for each location was extracted from the Harmonized World Soil Database (http://www.iiasa.ac.at/web/home/research/researchPrograms/water/HWSD.html). Relationships of N_{area} with V_{cmax} and R_d were also tested by OLS linear regression with or without LMA as an additional predictor. All regressions were performed in R (version 3.5.1).

Results

Testing the theoretical implications: thermal acclimation of R_d, V_{cmax} and their ratio

The predicted relationship of $V_{cmax,tg}$ to growth temperature (β_{aV}) was 5.5% K^{-1} under standard environmental conditions. The clear difference between the instantaneous sensitivities of leaf R_d and V_{cmax} to temperature implies that the sensitivity of acclimated $R_{d,tg}$ to temperature (β_{aR}) is 1.8% lower than that of $V_{cmax,tg}$ (β_{aV}), implying a theoretical optimum rate of increase of $R_{d,tg}$ by 3.7% K^{-1}. Despite the various simplifications we made, and large variation among species at any given site, these theoretical values are very close to the data-fitted values – whether obtained from all-species or site-mean analyses. They are however shallower than the 9.9% and 8.1% K^{-1} predicted for the instantaneous responses of V_{cmax} and R_d (Table 1, Fig. 2). In the all-species analysis, in spite of the large within-site spread, our theoretical predictions are indistinguishable from the fitted regression coefficients of normalized and transformed $V_{cmax,tg}$ and $R_{d,tg}$ against $mGDD_0$ (5.2 ± 0.3% K^{-1}, R^2 = 0.48 for $V_{cmax,tg}$, and 3.3 ± 0.2% K^{-1}, R^2 = 0.34 for $R_{d,tg}$) (Table 1, Fig. 2). Growth temperature alone explains 45% and 65% of observed the site-mean variation in $V_{cmax,tg}$ and $R_{d,tg}$ respectively (Table S1, Fig. S3).

Quantity	Theoretical value	Fitted coefficient	Confidence intervals		Intercept (mean ± se)	R^2	*df*
			2.5%	97.5%			
$R_{d,tg}$	0.037	0.033	0.029	0.038	–9.335±0.051	0.34	1245
$V_{cmax,tg}$	0.055	0.052	0.047	0.057	–6.255±0.054	0.48	1009
$R_{d,tg}/V_{cmax,tg}$	–0.018	–0.017	–0.023	–0.011	–3.044±0.061	0.03	1007
$R_{d,25}$	–0.044	–0.049	–0.054	–0.045	–7.261±0.052	0.25	1245
$V_{cmax,25}$	–0.044	–0.042	–0.047	–0.036	–3.922±0.054	0.25	1009
$R_{d,25}/V_{cmax,25}$	0	–0.007	–0.012	0.001	–3.302±0.060	0.00	1007

Table 1: Summary of Ordinary Least-Squares regressions for natural log-transformed leaf R_d and V_{cmax}, and their ratio as a function of growth temperature. Both R_d and V_{cmax} have been converted to growth temperature ($R_{d,tg}$ and $V_{cmax,tg}$) and to 25˚C ($R_{d,25}$ and $V_{cmax,25}$) from the measured leaf temperature, and normalized by site-mean leaf absorbed photosynthetic photon flux density. For comparison, the theoretical values of thermal sensitivities are shown together with the fitted coefficient and its confidence intervals. Non-significant coefficients are shown in grey.

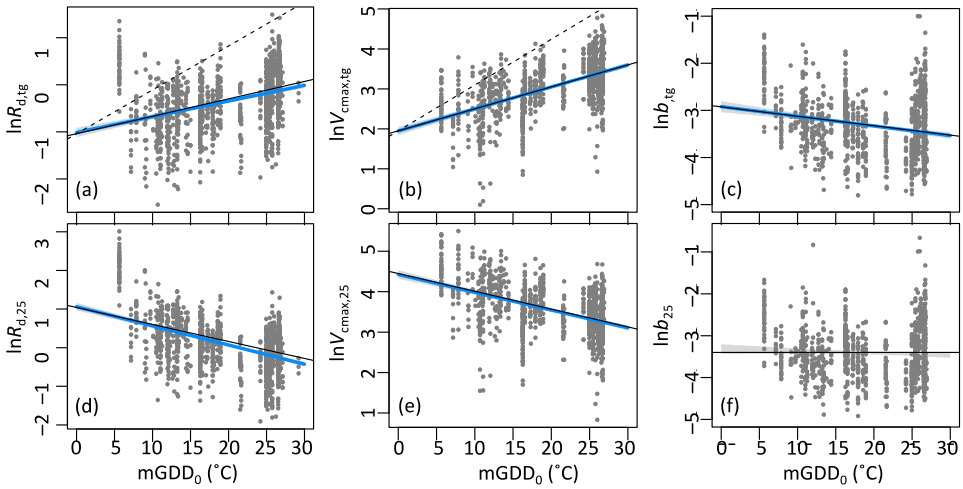

Figure 2: Natural log-transformed R_d, V_{cmax} and their ratio as a function of growth temperature. Both R_d and V_{cmax} are standardized to growth temperature and to 25˚C, and normalized by site-mean leaf absorbed photosynthetic photon flux density. Solid blue lines are the fitted lines from Ordinary Least Squares regressions. Solid black lines are theoretical predictions. Dashed lines represent instantaneous temperature responses, referenced to 0 °C.

Theoretically predicted values of the fractional sensitivities of acclimated $R_{d,25}$ (β_{aR25}) and $V_{cmax,25}$ (β_{aV25}) to temperature are negative (–4.4 % K^{-1}) and this is consistent with the observed negative responses of $R_{d,25}$ and $V_{cmax,25}$ to temperature seen in the data (Table 1). The observed negative response of $V_{cmax,25}$ to growth temperature is indistinguishable (–4.2 ± 0.3% K^{-1} for all-species, –3.4 ± 0.9% K^{-1} for site-mean) from our theoretical prediction, while the observed response of $R_{d,25}$ is marginally larger than our all-species prediction (–4.9 ± 0.3% K^{-1}), but indistinguishable in the site-mean analysis (–4.3 ± 0.7% K^{-1}).

Regressions performed without PPFD-normalization showed temperature responses with the same signs (positive for V_{cmax} and R_d at growth temperature, negative at 25˚C) but slightly steeper (positive slopes) or shallower (negative slopes) than in the main analyses (Table S2) – as expected due to the confounding of PPFD and temperature effects (Fig. S2), which normalization removes. R^2 values were consistently greater in the main analyses, by 6-7% for V_{cmax} and R_d at growth temperature and 11-17% for V_{cmax} and R_d at 25˚C.

Mixed-effects models show a similar acclimation pattern to the OLS regression models (Table S3). When the random effect from either species or site effect is included excluded, the predicted positive (but weaker than instantaneous) thermal responses of $R_{d,tg}$ and $V_{cmax,tg}$ emerge from the data. The resulting negative thermal responses of $R_{d,25}$ and $V_{cmax,25}$ are also supported by the data. The data-fitted thermal sensitivities after acclimation show patterns in agreement with our theoretical predictions ($\beta_{aR} < \beta_{aV}$ whereas $\beta_{aR25} = \beta_{aV25}$), although the fitted sensitivities in these analyses are marginally higher than the theoretical predictions (Table S3).

Using only a subset of the dataset with no temperature correction applied to the measured R_d and V_{cmax}, we again show thermal acclimation of $R_{d,25}$ and $V_{cmax,25}$ consistent with our prediction. Although the responses of $R_{d,gt}$ and $V_{cmax,gt}$ to growth temperature in this analysis are stronger than predicted, the uncertainties are much larger due to the limited size of this subset (Table S4).

Regressions based on the GlobResp and LCE datasets separately are generally consistent with our theoretical predictions (Table S5). The LCE dataset shows a stronger acclimation in $R_{d,tg}$ and a weaker acclimation in $R_{d,25}$ than V_{cmax} ($\beta_{aR} > \beta_{aV}$, $\beta_{aR25} < \beta_{aV2}$), but the empirically estimated sensitivities are nevertheless close to our theoretical predictions.

The prediction that b should decline with temperature by 1.8% K^{-1} was consistent with the fitted regressions of the ratio of $R_{d,tg}$ to $V_{cmax,tg}$; we observed a small but significant negative response of b to growth temperature with a sensitivity of 2.0% ± 0.3%, while b_{25} was indeed independent of $mGDD_0$ (Table 1, Table S3, Fig. 2). The fitted temperature response of $R_{d,tg}$ was consistently about 2% less steep than that of $V_{cmax,tg}$ (Table 1). However, the observed temperature-dependence of this ratio is weak and

becomes nonsignificant in analysis of site-mean data or the LCE dataset alone (Table S1, S3, S5).

Testing the theoretical assumptions: relationships of dark respiration and photosynthetic capacity to other variables

We examined the relationships between R_d, V_{cmax} and other potential influences, in order to further test our assumption that among those variables that measured R_d is most strongly correlated to variations in V_{cmax}. We found that measured R_d and V_{cmax} were positively correlated in the datasets when normalized either to $mGDD_0$ (R^2 = 0.25) or to a reference temperature of 25˚C (R^2 = 0.16) (Table S6). The canonical value of b_{25} = 0.015 in the photosynthesis model of Collatz et al. (1991), was similar to the fitted value of b_{25} = 0.014 ± 0.001 based on the regression of $R_{d,25}$ with respect to $V_{cmax,25}$ (Table S6).

Considered on their own, neither LMA nor soil pH provided explanatory power in the variations of leaf R_d and V_{cmax} (whether at 25˚C and growth temperature). The inclusion of one or the other in addition to $mGDD_0$ as a predictor provided negligible increases in explained variance (Table S7).

Relationships of leaf R_d and V_{cmax} to N_{area} were similar in strength when normalized to 25˚C (R^2 = 0.14 and 0.12) (Table 2), but notably weaker when considered at growth temperature (R^2 = 0.05 for $R_{d,tg}$ and 0.02 for $V_{cmax,tg}$). LMA and $V_{cmax,25}$ together accounted for 42% variation in N_{area}, but most of this explanatory power comes from LMA (Table 2). LMA and $R_{d,25}$ together explained 41% variation in N_{area}, but again most of this explanatory power is due to LMA (Table 2).

Coefficient					Intercept	R^2	*df*
$V_{cmax,tg}$	$V_{cmax,25}$	$R_{d,tg}$	$R_{d,25}$	LMA			
0.083±0.019					0.409±0.059	0.02	935
0.058±0.015				0.491±0.021	–1.849±0.107	0.39	934
	0.242±0.022				–0.199±0.081	0.12	935
	0.148±0.018			0.458±0.021	–2.055±0.106	0.42	934
		0.177±0.022			0.677±0.015	0.05	1165
		0.107±0.018		0.508±0.020	–1.724±0.097	0.38	1164
			0.301±0.022		0.590±0.013	0.14	1165
			0.174±0.019	0.471±0.020	–1.606±0.097	0.41	1164

Table 2: Summary statistics for Ordinary Least Squares regressions of leaf nitrogen content against leaf mass per area (LMA) and/or R_d or V_{cmax}. R_d and V_{cmax} are assessed at growth temperature ($R_{d,tg}$ and $V_{cmax,tg}$), or 25˚C ($R_{d,25}$ and $V_{cmax,25}$). The fitted slopes are shown together with the intercept (mean ± standard error), the adjusted coefficient of determination (R^2) and the degrees of freedom (*df*). All variables were natural-log transformed.

Discussion

Comparison with other studies

Heskel et al. (2016) provided an empirical function for leaf R_d at 25˚C (equation (4) in Methods), where the parameter a (the logarithm of the basal rate of R_d at 0˚C) is –1.60 for tundra, declining to –2.75 for lowland tropical rainforest. We estimated a by rearranging equation (3) in Heskel et al. (2016) at a reference temperature of 25˚C, and assuming proportionality between $R_{d,25}$ and $V_{cmax,25}$, yielding independent estimates: a = –1.41 for tundra, and –2.50 for lowland tropical rainforest. The values of a given by Heskel et al. (2016) allow us to approximate the thermal sensitivity of a as –4.6% K^{-1}, assuming a growth temperature range of 25˚C from tundra to rainforest: close to our prediction, β_{qR} = –4.4% K^{-1}.

Our results are consistent with previous findings showing that while $V_{cmax,tg}$ increases with growth temperature, $V_{cmax,25}$, the amount of Rubisco, and the fraction of leaf N allocated to Rubisco all decline (Scafaro et al., 2017). We also found a small but significant negative response of $R_{d,tg}/V_{cmax,tg}$ to growth temperature (2.0% ± 0.3% K^{-1}) (Fig. 2), while $R_{d,25}/V_{cmax,25}$ was not significantly related to growth temperature (Fig. 2).

The canonical ratio $R_{d,25}/V_{cmax,25}$ = 0.015 (Collatz et al., 1991) perhaps co-incidentally lies within the 95% confidence intervals of the fitted slope (0.014 ± 0.001) obtained by regression of $R_{d,25}$ on $V_{cmax,25}$ (Table S6). Our theory predicts a temperature dependence of the ratio of $R_{d,gt}$ to $V_{cmax,gt}$ due to their different instantaneous thermal responses, and this is observed, but the relationship to temperature is much less robust than that of R_d and V_{cmax} themselves.

Implications of photosynthetic and respiratory acclimation

We predicted that field-measured $V_{cmax,tg}$ and $R_{d,tg}$ should increase with growth temperature by 5.5% and 3.7% per degree, respectively (Table 1, Fig. 2). These

responses are not instantaneous biochemical responses. They arise, instead, because of the differential temperature sensitivities of two quantities – the effective Michaelis-Menten coefficient of Rubisco (K) and the photorespiratory CO_2 compensation point (I^*) (see Methods). These predicted thermal sensitivities (β_{aV}, β_{aR}) are within the 95% confidence intervals of regression coefficients independently derived from data (Table 1, Fig. 2).

Many ecosystem and land-surface models disregard acclimation, and assume that the long-term R_d and V_{cmax} responses to temperature follow the instantaneous functions routinely observed (β_{iV} = 9.9% K^{-1} (Kattge & Knorr, 2007) and β_{iR} = 8.1% K^{-1} (Heskel et al., 2016). Our results contradict this assumption, and provide a quantification of the temperature responses of both V_{cmax} and R_d that explicitly takes acclimation into account. Given that V_{cmax} has been found to vary seasonally, and can be predicted using the temperature of previous week (Smith & Dukes, 2018), a weekly to monthly acclimation time scale would be appropriate for LSMs to incorporate this process. It has also been shown that high growth temperature has a stronger negative impact on the instantaneous thermal response of V_{cmax} than on dark respiration (Smith & Dukes, 2017b). However, such effects occur above 30˚C, whereas the maximum growth temperature of the sampled sites we used here is only ~28˚C. More measures at hot sites would be helpful for future studies to understand acclimation behaviour over a large range of temperatures.

Theory also predicts that the amount of active Rubisco should decline with temperature (β_{qV} = –4.4% K^{-1}), because the instantaneous response of V_{cmax} to temperature is steeper than its acclimated response. At higher temperatures, less active Rubisco is required to achieve the value of V_{cmax} indicated by the co-ordination hypothesis (Fig. 1). Lower levels of Rubisco require lower levels of maintenance respiration for Rubisco turnover. Both predictions are quantitatively consistent with observed negative responses of $R_{d,25}$ and $V_{cmax,25}$ to temperature (Table 1, Fig. 2), although the goodness of fit to the data at 25˚C is weaker than that at growth temperature.

The growth temperature-dependent trend in both V_{cmax} and leaf R_d emerges clearly from the data despite considerable scatter around the regression (Fig. 2). Much of this scatter may be linked to within-site microclimatic variation (especially in PPFD) that is not accounted for in analyses of this kind. Consistent with this hypothesis, growth

temperature explains a larger fraction of the variation in community-mean values of V_{cmax} and R_d (Table S1) than in individual species values. The diversity among species in other relevant traits and leaf life history may also explain some within-site variation in V_{cmax} and R_d. For example, it has been shown that diverse hydraulic strategies can influences plant photosynthetic capacity under the same abiotic conditions (Zhu et al., 2018), while age-dependent leaf physiology can significantly influence V_{cmax} and consequently the total canopy carbon uptake in tropical evergreen forests (Albert et al., 2018). Optimality-based theory on respiration acclimation as presented here could (a) be applied globally at a community-mean level, and (b) potentially be refined by explicitly considering variations within the canopy in microclimate and differences among plant strategies and leaf life histories.

Equation (3) could potentially allow predictions of the responses of leaf R_d to other environmental determinants, including vapour pressure deficit, elevation and CO_2. Our theory predicts a downregulation in V_{cmax} and thus in R_d (both at 25˚C and Tg) as a response to increased atmospheric CO_2. Consequently, enhanced thermal acclimation in V_{cmax} and R_d (β_{aV} = 2.7% K^{-1} and β_{aR} = 4.5% K^{-1}, $\beta_{qV} = \beta_{qR}$ = –5.4% K^{-1}) are expected at high CO_2. The data currently available do not allow us to test these predictions, for various reasons including (a) the limited environmental range covered by data, (b) correlations between potential explanatory variables and (c) uncertainties in the measurement methods used in manipulative experiments (Ainsworth & Long, 2005). Nevertheless, our theory provides testable predictions on the acclimation of R_d to various environmental factors and also a simple, first-principles approach to directly predict the thermal acclimation of R_d, which is one of the most important mechanisms missing from current LSMs (Huntingford et al., 2017).

On the correlation between R_d and N_{area}

Empirical relationships of both $V_{cmax,25}$ and $R_{d,25}$ to area-based leaf nitrogen content (N_{area}) have been interpreted as showing 'nitrogen limitation' at the leaf level (Luo et al., 2004) and form the basis of R_d prediction in some N-cycle enabled LSMs. However, recent studies have shown two problems with this interpretation. First, $V_{cmax,25}$ accounts for only the metabolic component of N_{area}, whereas a large component of variation in N_{area} is proportional to LMA (Dong, Prentice, Harrison, et al., 2017; Onoda et al., 2017). Here, we confirm that substantially more variation in N_{area} can be explained by LMA

than by V_{cmax} or R_d. This finding suggests that N_{area} is not the main determinant of either V_{cmax} or R_d (Table 2). Second, global patterns of variation in V_{cmax} have been shown to be predictable from climate alone (Smith, Keenan, Prentice, Wang, Wright, Niinemets, Crous, Domingues, Guerrieri, Ishida, et al., 2019), suggesting that $V_{cmax,25}$ (and therefore $R_{d,25}$) is not determined by N_{area}, but rather primarily by photosynthetic demand – which is set by the local climatic environment. This demand in turn determines the metabolic component of N_{area}. Differences in soil N availability then primarily influence plant-level carbon allocation, instead of leaf-level N: the less soil N supply, the more carbon allocated belowground for N acquisition (LeBauer & Treseder, 2008; Poorter et al., 2012).

Our analysis therefore suggests an alternative to the common approach to carbon-nitrogen cycle coupling in in LSMs, whereby leaf nitrogen is prescribed by plant functional types and used to predict V_{cmax} and leaf R_d at standard temperature, and enzyme kinetics determines their temperature response at both fast (half-hourly) and slower (weekly and longer) time scales. In our proposed approach, leaf nitrogen is determined jointly by LMA (which may differ among plant functional types) and V_{cmax}; V_{cmax} and R_d at standard temperature would then be considered independent of plant functional type, but allowed to acclimate gradually to environmental conditions following a simple optimality principle; and nitrogen availability would influence primarily the allocation of carbon to leaves.

Conclusion

The theory developed here provides a first-principles approach to predicting the thermal acclimation of leaf R_d, a key process missing from current LSMs. According to both theory and data, the observed thermal acclimation of R_d follows the optimization of V_{cmax} as predicted by the coordination hypothesis. This acclimation dampens the instantaneous response of R_d to temperature and shows little influence from other factors. The discrepancy between thermal acclimation and instantaneous thermal response implies that both R_d or V_{cmax}, converted to 25˚C or any other arbitrarily chosen reference temperature, must decline with plant growth temperature. These principles would be straightforward to incorporate in an LSM framework. The theory provides an explanation for observed correlations among N_{area}, V_{cmax} and R_d that differs from the

common assumption that N_{area} determines V_{cmax} and R_d, and supports an alternative perspective on the coupling between terrestrial carbon and nitrogen cycles.

Acknowledgements

This research was supported by National Key R&D Program of China (no. 2018YFA0605400), National Natural Science Foundation of China (no. 31600388) to H.W. and the High End Foreign Expert awards at Tsinghua University to I.C.P (GDW20181100161). It has received funding from the European Research Council (ERC) under the European Union's Horizon 2020 research and innovation programme (grant agreement No: 787203 REALM to I.C.P.) It is a contribution to the AXA Chair Programme in Biosphere and Climate Impacts and the Imperial College initiative on Grand Challenges in Ecosystems and the Environment. T.F.K acknowledges financial support from the Laboratory Directed Research and Development (LDRD) fund under the auspices of DOE, BER Office of Science at Lawrence Berkeley National Laboratory. O.K.A. acknowledges the support of the Australian Research Council (DP130101252 and CE140100008).

References

Ainsworth, E. A., & Long, S. P. (2005). What have we learned from 15 years of free-air CO_2 enrichment (FACE)? A meta-analytic review of the responses of photosynthesis, canopy properties and plant production to rising CO_2. *New Phytologist, 165*(2), 351-372.

Albert, L. P., Wu, J., Prohaska, N., de Camargo, P. B., Huxman, T. E., Tribuzy, E. S., . . . Smith, M. N. (2018). Age-dependent leaf physiology and consequences for crown-scale carbon uptake during the dry season in an Amazon evergreen forest. *New Phytologist, 219*(BNL-203201-2018-JAAM), 870–884.

Amthor, J. S. (2000). The McCree–de Wit–Penning de Vries–Thornley respiration paradigms: 30 years later. *Annals of Botany, 86*(1), 1-20.

Atkin, O. K., Bloomfield, K. J., Reich, P. B., Tjoelker, M. G., Asner, G. P., Bonal, D., . . . Cosio, E. G. (2015). Global variability in leaf respiration in relation to climate, plant functional types and leaf traits. *New Phytologist, 206*(2), 614-636.

Atkin, O. K., Bruhn, D., & Tjoelker, M. G. (2005). Response of Plant Respiration to Changes in Temperature: Mechanisms and Consequences of Variations in Q10; Values and Acclimation. In R.-C. M. Lambers H (Ed.), *Plant Respiration, Advances in Photosynthesis and Respiration* (Vol. 18, pp. 95–135). Springer, Dordrecht, The Netherlands.

Atkin, O. K., Millar, A. H., Gardeström, P., & Day, D. A. (2000). Photosynthesis, carbohydrate metabolism and respiration in leaves of higher plants. In *Photosynthesis* (pp. 153-175): Springer.

Atkin, O. K., Scheurwater, I., & Pons, T. L. (2007). Respiration as a percentage of daily photosynthesis in whole plants is homeostatic at moderate, but not high, growth temperatures. *New Phytologist, 174*(2), 367-380.

Atkin, O. K., & Tjoelker, M. G. (2003). Thermal acclimation and the dynamic response of plant respiration to temperature. *Trends in plant science, 8*(7), 343-351.

Bernacchi, C., Singsaas, E., Pimentel, C., Portis Jr, A., & Long, S. (2001). Improved temperature response functions for models of Rubisco-limited photosynthesis. *Plant, Cell & Environment, 24*(2), 253-259.

Bouma, T. J. (2005). Understanding plant respiration: separating respiratory components versus a process-based approach. In *Plant respiration* (pp. 177-194): Springer.

Burnett, A. C., Davidson, K. J., Serbin, S. P., & Rogers, A. (2019). The "one-point method" for estimating maximum carboxylation capacity of photosynthesis: A cautionary tale. *42*(8), 2472-2481. doi:10.1111/pce.13574

Cannell, M., & Thornley, J. (2000). Modelling the components of plant respiration: some guiding principles. *Annals of Botany, 85*(1), 45-54.

Chen, J.-L., Reynolds, J. F., Harley, P. C., & Tenhunen, J. D. (1993). Coordination theory of leaf nitrogen distribution in a canopy. *Oecologia, 93*, 63-69.

Ciais, P., Sabine, C., Bala, G., Bopp, L., Brovkin, V., Canadell, J., . . . Heimann, M. (2014). Carbon and other biogeochemical cycles. *Climate change 2013: the physical science basis. Contribution of Working Group I to the Fifth Assessment Report of the Intergovernmental Panel on Climate Change*, 465-570.

Collatz, G. J., Ball, J. T., Grivet, C., & Berry, J. A. (1991). Physiological and environmental regulation of stomatal conductance, photosynthesis and transpiration: a model that includes a laminar boundary layer. *Agricultural and Forest meteorology, 54*(2-4), 107-136.

Cox, P. M., Betts, R. A., Jones, C. D., Spall, S. A., & Totterdell, I. J. (2000). Acceleration of global warming due to carbon-cycle feedbacks in a coupled climate model. *Nature, 408*(6809), 184-187.

Davis, T. W., Prentice, I. C., Stocker, B. D., Thomas, R. T., Whitley, R. J., Wang, H., . . . Cramer, W. (2017). Simple process-led algorithms for simulating habitats (SPLASH v. 1.0): robust indices of radiation, evapotranspiration and plant-available moisture. *Geoscientific Model Development, 10*(2), 689.

De Kauwe, M. G., Lin, Y.-S., Wright, I. J., Medlyn, B. E., Crous, K. Y., Ellsworth, D. S., . . . Domingues, T. F. (2016). A test of the 'one-point method' for estimating maximum carboxylation capacity from field-measured, light-saturated photosynthesis. *New Phytologist, 210*(3), 1130-1144. doi:10.1111/nph.13815

Dong, N., Prentice, I. C., Evans, B. J., Caddy-Retalic, S., Lowe, A. J., & Wright, I. J. (2017). Leaf nitrogen from first principles: field evidence for adaptive variation with climate. *Biogeosciences, 14*(2), 481-495.

Dong, N., Prentice, I. C., Harrison, S. P., Song, Q. H., & Zhang, Y. P. (2017). Biophysical homoeostasis of leaf temperature: A neglected process for vegetation and land-surface modelling. *Global Ecology and Biogeography, 26*, 998-1007.

Farquhar, G. D., von Caemmerer, S. v., & Berry, J. (1980). A biochemical model of photosynthetic CO_2 assimilation in leaves of C_3 species. *Planta, 149*(1), 78-90.

Galmés, J., Hermida-Carrera, C., Laanisto, L., & Niinemets, Ü. (2016). A compendium of temperature responses of Rubisco kinetic traits: variability among and within photosynthetic groups and impacts on photosynthesis modeling. *Journal of Experimental Botany, 67*(17), 5067–5091.

636 Galmés, J., Kapralov, M., Copolovici, L., Hermida-Carrera, C., & Niinemets, Ü.
637 (2015). Temperature responses of the Rubisco maximum carboxylase activity
638 across domains of life: phylogenetic signals, trade-offs, and importance for
639 carbon gain. *Photosynthesis Research, 123*, 183–201.
640 Gobron, N., Pinty, B., Taberner, M., Mélin, F., Verstraete, M. M., & Widlowski, J. L.
641 (2006). Monitoring the photosynthetic activity of vegetation from remote
642 sensing data. *Advances in Space Research, 38*(10), 2196-2202.
643 Harrison, S. P., Prentice, I. C., Barboni, D., Kohfeld, K. E., Ni, J., & Sutra, J. P. (2010).
644 Ecophysiological and bioclimatic foundations for a global plant functional
645 classification. *Journal of Vegetation Science, 21*(2), 300-317.
646 Haxeltine, A., & Prentice, I. C. (1996). A general model for the light-use efficiency of
647 primary production. *Functional Ecology, 10*(5), 551-561. doi:10.2307/2390165
648 Heskel, M. A., O'Sullivan, O. S., Reich, P. B., Tjoelker, M. G., Weerasinghe, L. K.,
649 Penillard, A., . . . Atkin, O. K. (2016). Convergence in the temperature response
650 of leaf respiration across biomes and plant functional types. *Proceedings of the*
651 *National Academy of Sciences, 113*(14), 3832-3837.
652 doi:10.1073/pnas.1520282113
653 Hoefnagel, M., Atkin, O., & Wiskich, J. (1998). Interdependence between chloroplasts
654 and mitochondria in the light and the dark. *Biochimica Et Biophysica Acta-*
655 *Bioenergetics, 1366*, 235-255.
656 Huntingford, C., Atkin, O. K., Heskel, M. A., Martinez-de la Torre, A., Harper, A. B.,
657 Bloomfield, K. J., . . . Mahli, Y. (2017). Implications of improved representation
658 of plant respiration in a changing climate. *Nature communications, 8*, 1602.
659 doi:10.1038/s41467-017-01774-z
660 Huntingford, C., Zelazowski, P., Galbraith, D., Mercado, L. M., Sitch, S., Fisher, R., .
661 . . Booth, B. B. (2013). Simulated resilience of tropical rainforests to CO_2-
662 induced climate change. *Nature Geoscience, 6*(4), 268.
663 Jenny, H. (1994). *Factors of soil formation: a system of quantitative pedology*: Courier
664 Corporation.
665 Kattge, J., & Knorr, W. (2007). Temperature acclimation in a biochemical model of
666 photosynthesis: a reanalysis of data from 36 species. *Plant, Cell &*
667 *Environment, 30*(9), 1176-1190.
668 Keenan, T. F., Prentice, I. C., Canadell, J. G., Williams, C. A., Wang, H., Raupach, M.,
669 & Collatz, G. J. (2016). Recent pause in the growth rate of atmospheric CO_2
670 due to enhanced terrestrial carbon uptake. *Nature communications, 7*, 13428.
671 LeBauer, D. S., & Treseder, K. K. (2008). Nitrogen limitation of net primary
672 productivity in terrestrial ecosystems is globally distributed. *Ecology, 89*(2),
673 371-379.
674 Luo, Y., Su, B., Currie, W. S., Dukes, J. S., Finzi, A., Hartwig, U., . . . Parton, W. J.
675 (2004). Progressive nitrogen limitation of ecosystem responses to rising
676 atmospheric carbon dioxide. *AIBS Bulletin, 54*(8), 731-739.
677 Maire, V., Martre, P., Kattge, J., Gastal, F., Esser, G., Fontaine, S., & Soussana, J.-F.
678 (2012). The coordination of leaf photosynthesis links C and N fluxes in C_3 plant
679 species. *PloS one, 7*(6), e38345.
680 New, M., Hulme, M., & Jones, P. (2000). Representing Twentieth-Century Space–
681 Time Climate Variability. Part II: Development of 1901–96 Monthly Grids of
682 Terrestrial Surface Climate. *Journal of Climate, 13*(13), 2217-2238.
683 Noguchi, K., & Yoshida, K. (2008). Interaction between photosynthesis and respiration
684 in illuminated leaves. *Mitochondrion, 8*, 87-99.

O'Leary, B. M., Asao, S., Millar, A. H., & Atkin, O. K. (2019). Core principles which explain variation in respiration across biological scales. *New Phytol.* doi:doi:10.1111/nph.15576

Onoda, Y., Wright, I. J., Evans, J. R., Hikosaka, K., Kitajima, K., Niinemets, Ü., . . . Westoby, M. (2017). Physiological and structural tradeoffs underlying the leaf economics spectrum. *New Phytologist, 214*(4), 1447-1463.

Poorter, H., Niklas, K. J., Reich, P. B., Oleksyn, J., Poot, P., & Mommer, L. (2012). Biomass allocation to leaves, stems and roots: meta-analyses of interspecific variation and environmental control. *New Phytologist, 193*(1), 30-50.

Prentice, I. C., Dong, N., Gleason, S. M., Maire, V., & Wright, I. J. (2014). Balancing the costs of carbon gain and water transport: testing a new theoretical framework for plant functional ecology. *Ecology letters, 17*(1), 82-91.

Prentice, I. C., Liang, X., Medlyn, B. E., & Wang, Y.-P. (2015). Reliable, robust and realistic: the three R's of next-generation land-surface modelling. *Atmospheric Chemistry and Physics, 15*(10), 5987-6005.

Reich, P. B., Sendall, K. M., Stefanski, A., Wei, X., Rich, R. L., & Montgomery, R. A. (2016). Boreal and temperate trees show strong acclimation of respiration to warming. *Nature, 531*(7596), 633-636.

Rogers, A. (2014). The use and misuse of $V_{c,max}$ in Earth System Models. *Photosynthesis Research, 119*, 15-29.

Scafaro, A. P., Xiang, S., Long, B. M., Bahar, N. H., Weerasinghe, L. K., Creek, D., . . . Atkin, O. K. (2017). Strong thermal acclimation of photosynthesis in tropical and temperate wet-forest tree species: the importance of altered Rubisco content. *Global Change Biology, 23*(7), 2783-2800.

Sinsabaugh, R. L., & Follstad Shah, J. J. (2012). Ecoenzymatic stoichiometry and ecological theory. *Annual Review of Ecology, Evolution, and Systematics, 43*, 313-343.

Slot, M., & Kitajima, K. (2015). General patterns of acclimation of leaf respiration to elevated temperatures across biomes and plant types. *Oecologia, 177*(3), 885-900.

Smith, N. G., & Dukes, J. S. (2017a). LCE: leaf carbon exchange data set for tropical, temperate, and boreal species of North and Central America. *Ecology, 98*(11), 2978-2978.

Smith, N. G., & Dukes, J. S. (2017b). Short-term acclimation to warmer temperatures accelerates leaf carbon exchange processes across plant types. *Global Change Biology, 23*(11), 4840-4853.

Smith, N. G., & Dukes, J. S. (2018). Drivers of leaf carbon exchange capacity across biomes at the continental scale. *99*(7), 1610-1620. doi:10.1002/ecy.2370

Smith, N. G., Keenan, T. F., Prentice, C. I., Wang, H., Wright, I. J., Niinemets, Ü., . . . Zhou, S.-X. (2019). Global photosynthetic capacity is optimized to the environment. *Ecology letters, 22*(3), 506-517. doi:10.1111/ele.13210

Smith, N. G., Keenan, T. F., Prentice, I. C., Wang, H., Wright, I. J., Niinemets, Ü., . . . Zhou, S.-X. (2019). Global photosynthetic capacity is optimized to the environment. *Ecology letters*. doi:10.1111/ele.13210

Smith, N. G., Malyshev, S. L., Shevliakova, E., Kattge, J., & Dukes, J. S. (2016). Foliar temperature acclimation reduces simulated carbon sensitivity to climate. *Nature Climate Change, 6*(4), 407-411.

Tcherkez, G., Boex-Fontvieille, E, Mahe, A, Hodges, M (2012). Respiratory carbon fluxes in leaves. *Current Opinion in Plant Biology, 15*, 308-314.

734 Tcherkez, G., Gauthier, P., Buckley, T. N., Busch, F. A., Barbour, M. M., Bruhn, D., .
735 . . Cornic, G. (2017). Leaf day respiration: low CO_2 flux but high significance
736 for metabolism and carbon balance. *New Phytol., 216*(4), 986-1001.
737 doi:doi:10.1111/nph.14816
738 Terrer, C., Vicca, S., Stocker, B. D., Hungate, B. A., Phillips, R. P., Reich, P. B., . . .
739 Prentice, I. C. (2018). Ecosystem responses to elevated CO2 governed by plant–
740 soil interactions and the cost of nitrogen acquisition. *New Phytologist, 217*(2),
741 507-522. doi:10.1111/nph.14872
742 Togashi, F. H., Prentice, I. C., Atkin, O. K., Macfarlane, C., Prober, S. M., Bloomfield,
743 K. J., & Evans, B. J. (2018). Thermal acclimation of leaf photosynthetic traits
744 in an evergreen woodland, consistent with the co-ordination hypothesis.
745 *Biogeosciences, 15*, 3461–3474.
746 Vanderwel, M. C., Slot, M., Lichstein, J. W., Reich, P. B., Kattge, J., Atkin, O. K., . . .
747 Kitajima, K. (2015). Global convergence in leaf respiration from estimates of
748 thermal acclimation across time and space. *New Phytologist, 207*(4), 1026-
749 1037.
750 Wang, H., Prentice, I., & Davis, T. (2014). Biophsyical constraints on gross primary
751 production by the terrestrial biosphere. *Biogeosciences, 11*(20), 5987-6001.
752 Wang, H., Prentice, I. C., Keenan, T. F., Davis, T. W., Wright, I. J., Cornwell, W. K., .
753 . . Peng, C. (2017). Towards a universal model for carbon dioxide uptake by
754 plants. *Nature plants, 3*(9), 734-741.
755 Wright, I. J., Reich, P. B., Atkin, O. K., Lusk, C. H., Tjoelker, M. G., & Mark, W.
756 (2006). Irradiance, temperature and rainfall influence leaf dark respiration in
757 woody plants: evidence from comparisons across 20 sites. *New Phytol., 169*(2),
758 309-319.
759 Wright, I. J., Reich, P. B., Westoby, M., Ackerly, D. D., Baruch, Z., Bongers, F., . . .
760 Diemer, M. (2004). The worldwide leaf economics spectrum. *Nature, 428*, 821-
761 827.
762 Zhu, S.-D., Chen, Y.-J., Ye, Q., He, P.-C., Liu, H., Li, R.-H., . . . Cao, K.-F. (2018).
763 Leaf turgor loss point is correlated with drought tolerance and leaf carbon
764 economics traits. *Tree physiology, 38*, 658–663.
765